ARTICLE

Land-use changes influence climate resilience through altered population demography in a social insect

Shih-Fan Chan[1,2,3] | Dustin R. Rubenstein[4,5] | Tsung-Wei Wang[1,6] | Ying-Yu Chen[1] | I-Ching Chen[7] | Dong-Zheng Ni[7] | Wei-Kai Shih[7] | Sheng-Feng Shen[1,2,3]

[1]Biodiversity Research Center, Academia Sinica, Taipei, Taiwan

[2]Department of Life Science, National Taiwan Normal University, Taipei, Taiwan

[3]Biodiversity Program, Taiwan International Graduate Program, Academia Sinica and National Taiwan Normal University, Taipei, Taiwan

[4]Department of Ecology, Evolution and Environmental Biology, Columbia University, New York, New York, USA

[5]Center for Integrative Animal Behavior, Columbia University, New York, New York, USA

[6]Institute of Ecology and Evolutionary Biology, National Taiwan University, Taipei, Taiwan

[7]Department of Life Sciences, National Cheng Kung University, Tainan, Taiwan

Correspondence
Sheng-Feng Shen
Email: shensf@sinica.edu.tw

Handling Editor: Jean-Philippe Lessard

Abstract

Biodiversity is threatened by both climate and land-use change. However, the synergistic impacts of these stressors and the underlying mechanisms remain poorly understood. This study seeks to bridge this knowledge gap by testing two competing hypotheses regarding the concept of the realized thermal niche. The Fixed Niche Breadth hypothesis suggests that a species' thermal niche remains constant despite fluctuations in population density resulting from land-use changes. This hypothesis links habitat loss directly to a reduced availability of suitable climate. Conversely, the Habitat Loss-Allee Effect hypothesis posits that land-use changes narrow the realized thermal niche by lowering population densities, which impairs individual fitness in unfavorable temperatures due to the Allee effect—the positive impact of higher population density on individual fitness. To investigate these hypotheses, we developed an individual-based model that integrates the Allee effect to examine how climate and land-use changes affect population density and the thermal niche in social organisms. We empirically tested our model predictions by studying the distribution and cooperative behavior of burying beetles (*Nicrophorus nepalensis*), which compete with blowflies for carrion resources, along two elevational gradients in Taiwan. These gradients serve as temperature gradients, one in an intact forest and the other in a human-altered landscape with substantial forest loss. Our results support the model predictions and show that landscape forest loss reduces beetle population densities and disrupts their dispersal dynamics, resulting in smaller cooperative groups. This, in turn, limits the beetles' ability to compete with blowflies in warmer environments, resulting in a contraction of the realized thermal niche. Together, our findings support the Habitat Loss-Allee Effect hypothesis while rejecting the Fixed Niche Breadth hypothesis. By highlighting the effects of habitat loss and fragmentation on both intra- and interspecific social interactions, our study improves understanding of species' vulnerability to the combined threats of climate and land-use change. Ultimately, our results underscore the importance of considering the demographic and behavioral consequences of land-use change when assessing species' vulnerability to climate-land-use synergies.

INTRODUCTION

Ongoing global climate change is causing dramatic biodiversity loss and species redistribution across the globe (Chen et al., 2011; Parmesan & Yohe, 2003; Pecl et al., 2017). The direct effects of climate change, including declines in local population abundance, local population extinction, and large-scale polar or upward shifts in distributional ranges have been widely explored (Parmesan, 2006). Furthermore, an increasing number of studies have focused on the interactions between climate and other biodiversity stressors (Brook et al., 2008), particularly anthropogenic land-use change, which also extensively reshapes global species distributions and ecosystem functioning (Foley et al., 2005; Haddad et al., 2015; Newbold et al., 2015). Accumulating evidence suggests that land-use change reinforces the negative impacts of climate change, resulting in deleterious impacts greater than the sum of the individual contributions of these two threatening processes (Elsen et al., 2020; Guo et al., 2018; Oliver et al., 2015; Oliver & Morecroft, 2014; Peters et al., 2019). Yet, the mechanism by which this interactive process works remains largely unexplored (Schulte to Bühne et al., 2021).

Most theories explaining how climate and land-use change synergistically affect organismal population abundance have been largely based on the assumption that an organism's climatic niche is not affected by land-use change. The idea for this comes from Hutchinson's distinction between niche and biotope (Colwell Robert & Rangel Thiago, 2009; Hutchinson, 1957). According to Hutchinson, the niche represents the *n*-dimension environmental attributes (e.g., temperature and humidity) required for species' positive population growth rate, whereas the biotope represents the physical space, such as the habitat in which organisms are distributed (Colwell Robert & Rangel Thiago, 2009). Land-use change reduces habitat (biotope) availability (Platts et al., 2019) and connectivity (Hof et al., 2011; Senior et al., 2019), and prevents organisms from tracking suitable climates (niche) to keep pace with temperature change (Travis, 2003; Tucker et al., 2018). Based on this niche theory, we propose the "Fixed Niche Breadth hypothesis," which posits that land-use change only affects habitat availability, leaving the niche breadth—determined by species' physiological and behavioral traits—unaffected, regardless of population density.

A rarely considered alternative to the Fixed Niche Breadth hypothesis is the Habitat Loss Allee Effect hypothesis. This hypothesis suggests that land-use change, after reducing available habitat and causing an initial reduction in population density, causes negative effects on social behaviors that are necessary for individual survival and reproduction, including mate searching (Wells et al., 1998), group foraging (Grünbaum & Veit, 2003), or cooperation (Courchamp et al., 1999). This inverse density-dependent relationship in which smaller population densities are associated with lower average individual fitness is often referred to as the Allee effect (Allee, 1927, 1931; Courchamp et al., 1999; Stephens & Sutherland, 1999), a hallmark of social species that form groups. The Allee effect driven by land-use change may thus reduce the realized thermal niche breadth by exacerbating the difficulty for organisms to find mates or cooperate in harsh environments (e.g., unfavorable temperatures). Consequently, land-use change may not only directly impact organisms by reducing the amount of suitable available habitats, but also by reducing the fitness of individuals living in the remaining pristine habitats in the local area. Yet, to our knowledge, no study has considered the possibility that in addition to affecting population density, reducing habitat may also affect niche breadth through Allee effects. Given the widespread occurrence of Allee effects across diverse animal species (Angulo et al., 2007, 2018; Courchamp et al., 1999; Stephens & Sutherland, 1999), the impact of land-use change on social organisms under climate change is likely to be underestimated.

To test the Fixed Niche Breadth and Habitat Loss-Allee Effect hypotheses, we first constructed a spatially explicit, individual-based model (IBM) to investigate how land-use change affects population density along a temperature gradient, which then further impacts the realized thermal niche in terms of distribution, population density, and breeding performance, of social organisms through the Allee effect. Complementing this theoretical approach, we conducted an empirical study centered on the Asian burying beetle (*Nicrophorus nepalensis*) along two elevational gradients in Taiwan, each characterized by varying degrees of land-use change and possible variations in environmental temperature. These beetles engage in intraspecific cooperation to compete against blowflies for their critical reproductive resources—vertebrate carcasses (Chen et al., 2020;

Scott, 1994, 1998; Sun et al., 2014). Such intraspecific cooperation typically involves multiple beetles working together to remove blowfly eggs and maggots from a carcass, as well as burying the carcass. This behavior is pivotal for their reproductive success, especially in warmer environments where the coexisting blowfly maggots are able to more effectively consume the carcasses (Liu et al., 2020; Sun et al., 2014; Tsai, Rubenstein, Chen, et al., 2020). We aim to test the hypotheses by examining how varying degrees of land-use change influence beetle population densities and cooperative behaviors along these elevational gradients. According to the Habitat Loss-Allee Effect hypothesis, we expect beetles in intact forests to exhibit higher population densities and higher levels of cooperation, potentially leading to a broader niche breadth, in contrast with those in human-altered landscapes where lower population densities and reduced cooperation are anticipated. In contrast, according to the Fixed Niche Breadth hypothesis, we predict similar thermal niche breadth in both intact and human-altered landscapes despite higher population densities in the former. By examining these competing hypotheses, we aim to improve our understanding of how climate and land-use change interact to shape species' realized thermal niches, contributing to a more comprehensive framework for predicting biodiversity responses to global change, and thereby informing conservation strategies.

MATERIALS AND METHODS

IBM to simulate the impact of land-use change on realized thermal niches

We developed an individual-based model (IBM) to examine the impact of land-use changes on the realized thermal niche of social organisms, as indicated by habitat occupancy, population density, and reproductive success
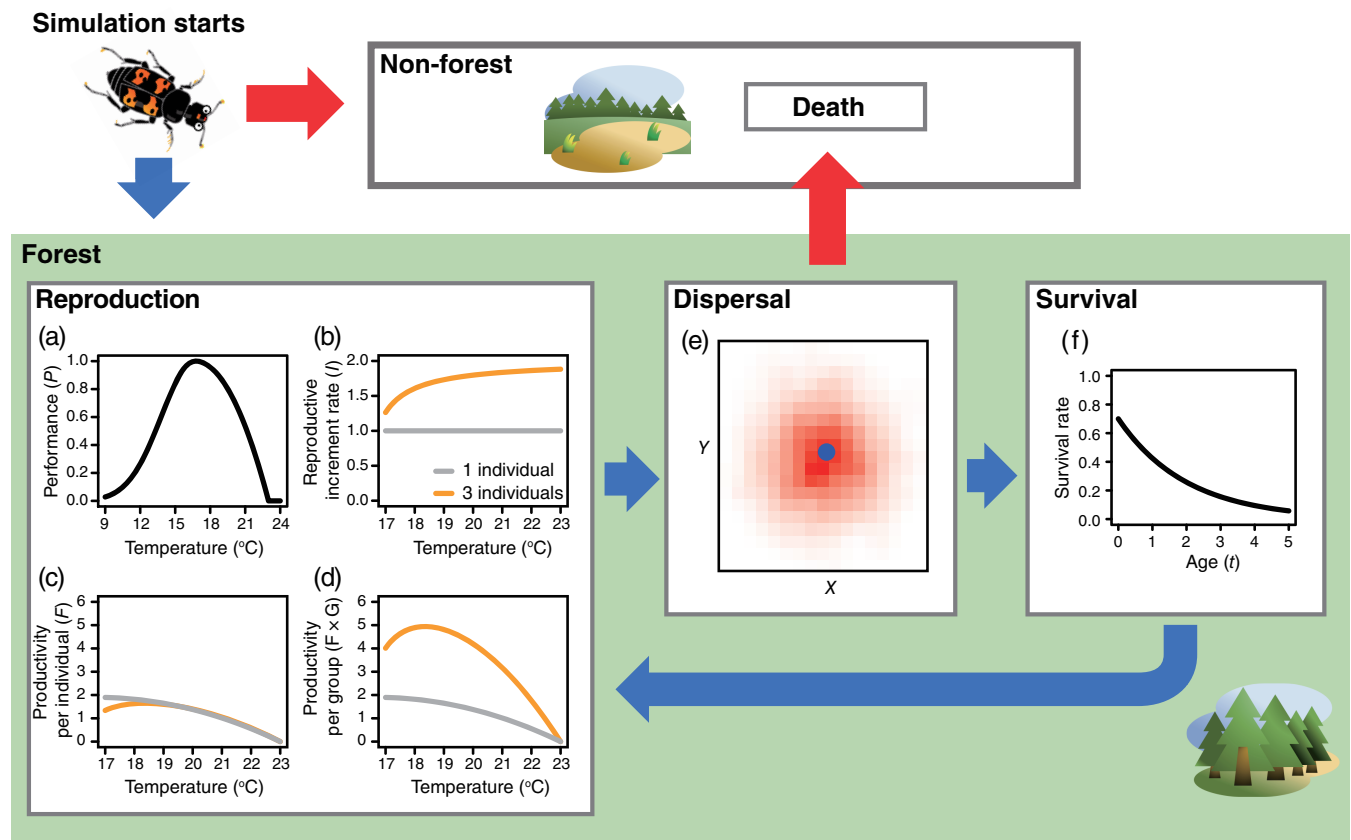

FIGURE 1 Flow chart of the individual-based model simulation process. At the start of each simulation, individuals located in non-forested habitats died immediately. However, individuals located in forested habitats underwent three sequential steps: Reproduction, dispersal, and survival. Individuals that dispersed to non-forested habitats also died. (a) The thermal performance curve used in the model. (b) Variation in cooperative benefits along the temperature gradient. (c) Variation in individual productivity in small and large groups along the temperature gradient. (d) Variation in group productivity in small and large groups along the temperature gradient. (e) The probability of post-natal dispersal to each grid modeled by a Gaussian kernel density function. (f) The relationship between individual survival rate and age. In (e), the blue dots indicate the birthplace of the focal individual. The higher the probability of dispersal to a location, the redder the color of the corresponding grid. Beetle illustration by Shih-Fan Chan.

along a temperature gradient, and thereby predict the interactions between climate and land-use change. The IBM simulates the processes of reproduction, dispersal, and mortality within both an undisturbed intact forest landscape and one altered by human activity (Figure 1). Crucially, the model accounts for temperature-dependent individual performance and the advantages of cooperative behavior during reproduction. Additionally, it considers the amplifying effect of local population density on the likelihood of cooperation. To discern the impact of social behavior, we also simulated nonsocial organisms as a control group, enabling a comparison of the outcomes.

We set a spatial range of 400 patches and randomly selected suitable forest habitats according to habitat availability. For intact forest landscapes, the habitat availability was set to 1, which means all 400 patches were forests. For human-altered landscapes, the habitat availability was set to 0.7, which means that 280 patches were randomly selected as forest habitat, and the rest of the patches were non-forest. For each simulation, the starting population size was set to 0.6 times the number of patches (i.e., 240 individuals), and was randomly distributed throughout the space.

At the start of the simulation, individuals that fall into the forest patches enter the step of reproduction. At each time step of the simulation, the breeding resources are presented randomly in 70% of the forest patches. Notably, only those individuals in suitable habitats with breeding resources have the opportunity to reproduce. Specific to the social species, individuals in the same patch produce group resources and reproduce when they occur in suitable habitats. However, in unsuitable habitats or habitats without breeding resources, individuals simply die and cannot reproduce. Therefore, reproductive output is set to zero in the simulation. For simplicity, we consider asexual reproduction.

To model asexual reproduction, we first modeled the effect of environmental temperature on the performance (P), which is the reproductive productivity of a solitary individual relative to its potential maximum productivity, using the thermal performance curve (TPC):

$$P(T) = \begin{cases} \exp\left(-\left((T - T_{\text{opt}})/2\sigma_p\right)^2\right), \text{when } T \leq T_{\text{opt}} \\ 1 - \left((T - T_{\text{opt}})/(T_{\text{opt}} - \text{CT}_{\max})\right)^2, \text{when } T > T_{\text{opt}} \end{cases}, \quad (1)$$

where T is the environmental temperature, σ_p is the shape parameter determining the steepness of the curve at the lower end, T_{opt} is the optimum temperature of the species, and $\text{CT}_{\max}$ is the critical thermal maximum of the species (Deutsch et al., 2008; Vasseur et al., 2014). We

assume that breeding performance is determined by the TPC when individuals reproduce solitarily (Figure 1a).

To incorporate the effect of group size on reproduction, we assume that cooperation enables individuals to improve their breeding performance, and because burying beetles experience greater interspecific competition from flies at higher temperatures (Liu et al., 2020; Sun et al., 2014), the benefit of cooperation is greater at higher temperatures (Figure 1b). To model this temperature-dependent cooperative benefit, we determined the overall increases in resource handling efficiency due to cooperation (E_c) by:

$$E_c = \begin{cases} 0, \text{when } G = 1 \\ \emptyset_K * G * b_K * \left(\dfrac{T - T_{\text{opt}}}{\text{CT}_{\max} - T_{\text{opt}}}\right), \text{when } G > 1 \end{cases}, \quad (2)$$

where $T > T_{\text{opt}}$ and $\emptyset_K$ denotes the proportion of energy an individual invests in cooperation, G denotes group size (number of individuals in each patch), and b_K denotes an increase in the resource handling efficiency of an individual by cooperation. Notably, for nonsocial species, $\emptyset_K = 0$ and hence $E_c = 0$.

As the group size grows too large, the cooperative benefits of the social species will eventually saturate and stop increasing (Figure 1b). To model this relationship, we determined the reproductive increment rate by cooperation (I) using a saturating function of E_c:

$$I = 1 + \frac{E_c}{K_s + E_c}, \quad (3)$$

where K_s is the half-saturation constant, which is the value of E_c at which the reproductive increment rate by cooperation (I) is half of its maximum. The equation determines an upper bound for the cooperative benefit. For nonsocial species, $I = 1$ as $E_c = 0$, which indicates no increment by cooperation.

Finally, we obtained the productivity of an individual (F) at a given environmental temperature (T) by:

$$F(T) = \frac{\alpha}{\sqrt{G}} \times P(T) \times I \times (1 - C\emptyset_K), \quad (4)$$

where α is the maximum productivity of a solitary individual, and C denotes the rate of cost of cooperation. This equation determines the relationship between the reproductive performance of individuals with the cooperative benefits at different environmental temperatures. When the environmental temperature exceeds an individual's physiologically optimal temperature, the breeding performance of individuals in a social group remains poor (Figure 1c), even when the cooperative benefits are high

(Figure 1b), and group productivity is higher in larger social groups (Figure 1d). However, specific to nonsocial species, productivity is solely governed by the TPC and the negative density-dependent regulation (i.e., the larger the group size, the lower the productivity) as $\emptyset_K = 0$ and $I = 1$.

After an individual produces offspring, those offspring randomly disperse into patches, which is modeled by a Gaussian kernel density function (Figure 1e). Finally, we determined the survival rate I of the individuals after dispersal by an exponential decay function (Figure 1f):

$$r = r_0 e^{-\frac{t}{\tau}}, \tag{5}$$

where r_0 denotes the initial survival rate, t refers to the number of survival steps experienced by an individual at the given time step, and τ is the exponential time constant that determines the decay rate of survival rates across ages.

For simplicity, we begin with a population that is composed entirely of either social or nonsocial individuals. As the impacts of land-use change that we want to investigate occur at ecological timescales, we do not consider the possibility that cooperative behavior can evolve. Instead, we assume that the degree of individual cooperation is fixed. Thus, the productivity of a group is mainly influenced by the group size within a patch and environmental temperature. More individuals produce more group resources until the size of the group is larger than the optimal size. We assume that environmental resources are finite, and therefore, cooperative groups cannot produce more group resources indefinitely. For simplicity, we only simulate the warm distribution boundary (i.e., low elevation) with this model, though we note that the results would be qualitatively similar if we simulate both the warm and cold (i.e., high elevation) distribution boundaries together. Thus, we only simulate a situation in which the ambient temperature is higher than the optimum temperature of the species (i.e., $T > T_{\text{opt}}$), adopting the TPC described in Equation (1). We set T_{opt} to 16.7°C and CT_{max} to 23.0°C, based on the published data of *N. nepalensis* (Chan, Rubenstein, Chen, et al., 2023). Although our model is parametrized based on the biology of *N. nepalensis*, we emphasize that it applies to any species (social or otherwise) whose temperature-dependent fitness components can be described by TPCs. Definitions and values for all parameters in our model are summarized in Appendix S1: Table S1.

The total time step of each simulation is 2000 to ensure that the system reaches a steady state. We record the final number of patches with individuals, the final population size and population density (i.e., the final population size/ the number of patches suitable for reproduction), and the number of offspring produced by an individual in each patch. We also calculate the per capita offspring production accordingly. We simulate the ambient temperature range of 17–23°C at 0.2°C intervals. For each ambient temperature, we repeat the simulation 200 times and calculate the mean and SD of the 200 results.

Field study to examine the effect of land-use change on the population density, elevational range, and realized thermal niche of burying beetles

Study area

We tested the key predictions of the two hypotheses by examining the elevational distribution and breeding performance of the Asian burying beetle (*N. nepalensis*) along two elevational gradients on the eastern and western slopes of Mt. Hehuan, Taiwan (3422 m, main peak at 24°11′ N, 121°17′ E; Figure 2). According to the Chelsa database at ~1 km resolution (Karger et al., 2017), the mean annual temperature is 6.15°C at the summit, 22.75°C at the base of the eastern slope and 22.05°C at the western slope. The mean annual precipitation is 3045 mm at the summit, 3260 mm at the base of the eastern slope, and 2899 mm at the western slope. Below 1400 m above sea level (asl), pristine forests are dominated by evergreen broadleaf trees from the *Fagaceae*, *Lauraceae*, and *Theaceae* families. Above this elevation, mixed forests occur, characterized by the coexistence of conifers, including *Chamaecyparis*, *Picea*, and *Tsuga* species, with broadleaf trees such as *Beilschmiedia*, *Castanopsis*, *Cinnamomum*, and *Cyclobalanopsis* species. At elevations above 2500 m asl, the forest composition shifts predominantly to conifers such as *Abies kawakamii* and *Tsuga chinensis* var. *formosana* (Li et al., 2013). The eastern slope of the mountain is located within Taroko National Park and is covered by well-protected intact forest landscapes. In contrast, the forest on the western slope of Mt. Hehuan is highly fragmented and suffering from severe land conversion from forests to farmlands for agriculture and tourism, particularly at lower elevations where human activities are more intensive. The contrasting landscapes along the two slopes enable us to test how land-use change modulates the thermal niche and elevational distribution of the burying beetles.

Study species

Burying beetles rely exclusively on vertebrate carcasses for reproduction (Scott, 1998). However, a carcass is also a "bonanza resource" that is intensely competed for by
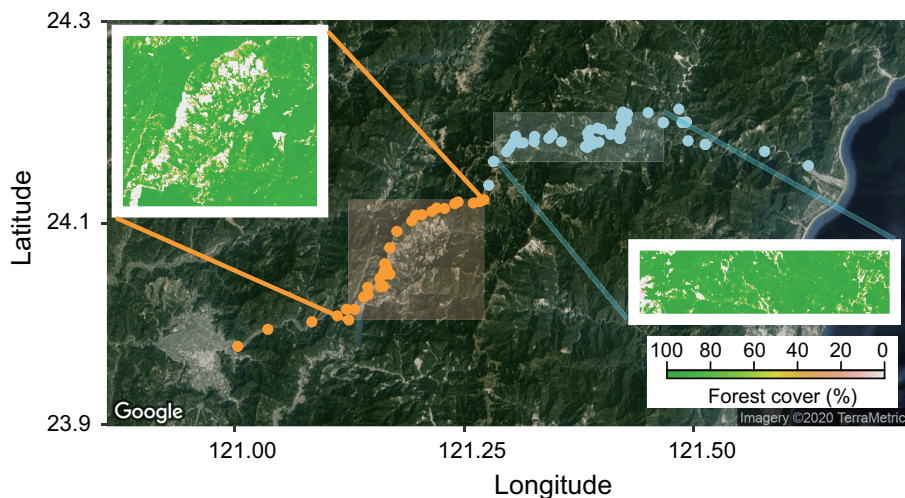
FIGURE 2 Study area. The satellite image for the study area is obtained from Google Maps. The orange and light blue dots represent the sampling sites along the western and eastern slopes of Mt. Hehuan, respectively. The semitransparent rectangular areas represent the regions where we conducted the breeding experiments. The insets indicate the distribution of forest cover in the semitransparent rectangular areas.

various necrophagous species (Wilson, 1975). The reproductive success of *N. nepalensis* is strongly limited by interspecific competition for these resources, especially from blowflies (Chan et al., 2019; Chen et al., 2020; Scott, 1994; Sun et al., 2014). *N. nepalensis* overcomes the challenge of interspecific competition with blowflies through intraspecific cooperation, which allows the beetles to successfully reproduce in warmer environments at lower elevations characterized by stronger blowfly competition (Liu et al., 2020; Sun et al., 2014; Tsai, Rubenstein, Chen, et al., 2020). Intraspecific cooperation thus helps the burying beetles to expand their thermal niche from cooler environments at higher elevations where blowflies are scarce or absent to warmer environments at lower elevations where blowflies are more abundant. Furthermore, the reproductive success of *N. nepalensis* is also limited by its ability to locate carcasses, especially in colder environments at higher elevations where extended movement is costly (Chan et al., 2019; Liu et al., 2020).

Field surveys and experiments with burying beetles

Our field study consisted of three major parts: (1) field surveys for beetle distribution and population density covering the entire elevational gradients; (2) field breeding experiments accessing the in situ reproductive success of burying beetles; and (3) manipulative field experiments examining the effect of beetle group size on their reproductive success. We conducted both types of breeding experiments within the elevational range of the

beetles observed in the density surveys. However, to understand the dynamics across range boundaries, we also conducted these experiments at sites slightly below the lower range boundaries. Some of the data from these surveys and experiments, conducted as part of our long-term burying beetle research project, have already been published (see later sections for specific references). In addition, we also integrated new information extracted from experimental videos and georeferenced databases to address the research question presented in this study.

Beetle population densities

We surveyed the population densities of burying beetles by setting up hanging pitfall traps ($n = 372$; Appendix S1: Table S2) at 71 sites, each sampled 1–16 times (median = 4; Appendix S1: Figure S1a), along the two elevational gradients: 124–3209 m asl on the eastern slope ($n = 224$ at 43 sites), and 500–3275 m asl on the western slope ($n = 148$ at 28 sites), with elevation intervals c.a. 100 m (median = 75 m). The surveys on the western slope descended to a minimum elevation of 500 m asl, as the terrain beneath this threshold levels out and gives way to urban areas with prevalent human activities. However, this survey range has sufficiently encompassed the lower elevational range boundary of the beetles. We conducted these surveys from June to September 2014 to 2015. The dataset was also analyzed in Chan et al. (2019) and Liu et al. (2020) previously for other research purposes. The hanging pitfall trap consists of a plastic bottle containing 100 g of rotten pork bait, a landing platform for beetles, and a roof to prevent rainfall (Chan et al., 2019; Liu et al., 2020; Tsai, Rubenstein, Fan, et al., 2020). We hung each trap in a tree at 1–1.5 m

above the ground, retrieved it after four nights, and calculated the number of burying beetles as our measure of population density.

Beetle reproductive success

We conducted breeding experiments to test the breeding performance of the beetles in pristine forests ($n = 392$; Appendix S1: Table S2) at 53 sites, each sampled 1–25 times (median = 6; Appendix S1: Figure S1b), along the two elevational gradients: 1166–2903 m asl on the western slope ($n = 176$ at 23 sites) and 1173–2838 m asl on the eastern slope ($n = 216$ at 30 sites), with elevation intervals c.a. 100 m (median = 61 m). We conducted these experiments from June to September 2012 to 2015. Samples collected between June and September 2013–2015 ($n = 299$) were gathered in a prior study (Chan et al., 2019) and were also analyzed in Liu et al. (2020) and Tsai, Rubenstein, Chen, et al. (2020). However, for the purposes of this study, we took additional measurements from the video recordings and considered additional environmental variables measured in the field. Each experimental set-up consisted of a plastic pot filled with soil, covered by a 2×2 cm wire mesh cage to exclude mammalian scavengers (Chan et al., 2019; Liu et al., 2020; Tsai, Rubenstein, Chen, et al., 2020). We provided a 75 g carcass of a domesticated feeder rat as bait (i.e., breeding resource) in the soil-filled pot. Such a design allows burying beetles and blowflies in the environment to freely access the carcass and reproduce. We visited each trial daily until the carcass was buried by the beetles, decomposed by microbial activity, or consumed by blowfly maggots and other insects (Chan et al., 2019). Once the carcass was buried by the beetles, we visited the trial after a further 14 days to determine the beetles' breeding success (i.e., the presence of third-instar larvae).

We also monitored each experiment with a surveillance camera and a digital video recorder (DVR). We set the camera on the wire mesh with the lens pointing down and the field of view covering the entire soil surface inside the pot to record burying beetle activity around and on the surface of the carcass. We identified the burying beetles' arrival day (i.e., the day of the first arrival) and group size (i.e., the average number of beetles at 22:00, 01:00, and 04:00 on the first night that the beetles appeared on the carcass; Liu et al., 2020). To estimate the potential intensity of competition from blowflies, we also quantified the abundance of blowflies on the carcasses (i.e., the average number of blowflies counted per 2 h on the first day; Chan et al., 2019; Chen et al., 2020) from the videos.

To test the influence of beetle population density on breeding performance, we also surveyed the population density at each site before and after each breeding experiment was carried out in 2014 and 2015 ($n = 323$). We estimated the population density at the beginning of each breeding experiment through linear interpolation by the time between the densities observed before and after the experiment. To prevent mutual interference, successive surveys and experiments in the same location were temporally separated with a minimum of a 4-day interval.

Manipulative experiments for population density

As higher population densities potentially enable beetles to form larger breeding groups, we tested whether increasing the group size through manipulation in the field can promote reproductive success in the human-altered landscape, specifically at low elevations on the western slope. We conducted these experiments from June to September 2012 to 2015. We carried out the experiments in pristine forests ($n = 333$; high-density treatment: $n = 164$; low-density treatment: $n = 169$; Appendix S1: Table S2) at 44 sites, each sampled 1–11 times (median = 4; Appendix S1: Figure S1c), along the two elevational gradients: 1164–3000 m asl on the western slope ($n = 215$ from 28 sites) and 900–3100 m asl on the eastern slope ($n = 118$ from 16 sites). Samples collected in 2012 and 2013 ($n = 105$) were previously analyzed in Liu et al. (2020) and Sun et al. (2014). Additionally, the data collected in 2014 and 2015 ($n = 228$) were also analyzed in Tsai, Rubenstein, Chen, et al. (2020). Our experimental apparatus comprized an inner plastic container ($21 \times 13 \times 13$ cm, containing 10 cm depth of soil) placed within an outer plastic container ($41 \times 31 \times 21.5$ cm container, containing 11 cm depth of soil) (Appendix S1: Figure S2). We provided several entrances on the side wall of the inner container, which allow beetles to freely move between the two containers. The cap of the box was lifted 10 cm above the upper edge of the box to create entrances for blowflies. However, these entrances were also covered by iron mesh (2×2 cm cell sizes) to exclude mammalian scavengers. We set up extended eaves around the edge of the cap of the outer container to prevent wild beetles from flying into the container. We also smeared Vaseline on the extended eaves and the side wall of the outer container to prevent wild beetles from climbing into the container. This apparatus allows us to manipulate group size in the container by releasing a specific number of beetles into the container, without being interfered with by wild beetles. Finally, we also mounted a camera on the cap of the box, with the lens pointing downwards and the field of view covering the entire surface of the soil inside the inner plastic container, to record the activity of burying beetles and blowflies around and on the surface of the carcass.

For each set of the paired high- and low-density treatments, we set up two apparatuses as described above, each containing a 75 g carcass of a domesticated feeder rat for the beetles. We then released beetles into the

containers. One contained one male and one female (i.e., the low-density treatment), and the other contained three males and three females (i.e., the high-density treatment). We captured the beetles for each set of the paired trials from nearby sites using the same pitfall traps as for our density surveys. However, at low elevations on the western slope, where there were no beetle populations, we used beetles captured from the lowest elevation where beetles occurred. We marked all of the beetles on the elytron, the modified, hardened forewing that forms a protective cover over the hindwings, with a marker pen to ensure that we could identify any invading free-ranging (i.e., unmarked) beetles in the videos. To mimic arrival patterns at different elevations, we released the beetles into the experimental apparatus 1, 2, and 3 days after the beginning of each trial (i.e., placement of the rat carcass) at elevations of 1700–2000 m (low), 2000–2400 m (intermediate) and 2400–2800 m (high), respectively (Liu et al., 2020; Sun et al., 2014; Tsai, Rubenstein, Chen, et al., 2020). We also visited each trial daily, following the same protocols as the natural breeding experiments described above.

Forest cover

We obtained forest cover data from published global forest cover maps with a spatial resolution of 30 m (Hansen et al., 2013). We created a buffer of 1000 m radius around each sampling point (for both surveys and experiments; $n = 71$) and calculated the mean forest cover within the buffer.

Environmental temperature monitoring

To assess the impact of temperature on beetle density and reproductive success, we measured ambient temperature every 30 min during each survey and experimental trial. We used an iButton data logger (Maxim Integrated Products, Sunnyvale, CA, USA), positioned at a height of 1.25–1.5 m, which is the recommended level for weather stations to measure surface air temperatures (Jarraud, 2008), adjacent to the experimental setup. To avoid direct exposure to sunlight in the field, we shielded the loggers with PVC pipe (Jang et al., 2022). We determined the mean daily temperature by averaging the temperatures recorded during each survey period (4 full days each), natural experiment (ranging from 1 to 16 full days, depending on the length of the experiment), and manipulative experiment (ranging from 2 to 7 full days, depending on the length of the experiment).

To further investigate the effects of forest cover and elevation on mean daily temperature, we selected multiple study sites at different slopes and elevations during the 2014 and 2015 field seasons and recorded temperatures throughout the season. In 2014, we selected 24 sites (13 on the eastern slope and 11 on the western slope) and recorded daily temperatures from June to September; in 2015, we selected 32 sites (16 on the eastern slope and 16 on the western slope) and recorded temperatures from July to September. A total of 37 sites were sampled over the two years (19 on the eastern slope and 18 on the western slope), with 19 sites providing data for both years (10 on the eastern slope and 9 on the western slope). Sampling elevations ranged from 1033 to 3209 m asl on the eastern slope and from 1018 to 3096 m asl on the western slope. Following the same protocol described previously, we installed temperature loggers in each study site and recorded daily temperatures within the time periods (Appendix S1: Figure S3). We then calculated the mean daily temperature for each day and site to prepare for further analysis.

Data analysis

We conducted two complementary analytical approaches to analyze the relationships among variables. Initially, we applied regression-based analyses, including linear models (LM), linear mixed models (LMM), and generalized linear mixed models (GLMM), to analyze individual relationships. Subsequently, we utilized piecewise structural equation modeling (pSEM) (Lefcheck, 2016; Shipley, 2009) to construct and analyze the overall causal framework. This sequential approach allowed us to first determine the significance and strength of pairwise associations before integrating them into a comprehensive model of the system's dynamics.

First, we applied various regression-based analyses to account for different data structures. We utilized an LM to assess the impact of elevation on forest cover across different slopes. In addition, we used LMMs to assess how elevation and forest cover influence ambient temperature along the two gradients. We also used negative binomial GLMMs to examine the effects of elevation, temperature, and forest cover on burying beetle population densities. Furthermore, we implemented binomial GLMMs to determine the influence of population density, environmental factors (in the natural breeding experiments), and experimental treatments (in the manipulative experiments) on beetle breeding success. Finally, we also used LMMs to analyze how beetle population density influence group size and arrival day at carcasses. To meet the normality assumption, we utilized a square root function to transform forest cover, beetle group size, and beetle arrival day in the L(M)Ms. We carried out the LM

using the R package Stats (R Core Team, 2022), and the LMMs and GLMMs using the R package *lme4* (Bates et al., 2015).

For all the models, we included the main effects of all independent variables of interest simultaneously. However, for complex models involving interactions or quadratic terms of independent variables (e.g., elevation and temperature), we started with a full model and then sequentially eliminated non-significant ($p > 0.05$) quadratic terms and interactions to arrive at a parsimonious model. We used a dummy variable called "Region" to compare the slopes of the west (coded as 1) and east (coded as 0). To account for temporal variation, we included Julian date (defined as the continuous day count starting from January 1 as day 0) as a covariate in all LMMs and GLMMs. We included "sampling site" as a random factor in LMMs and GLMMs to account for repeated sampling at sites. For manipulative breeding experiments conducted in matched pairs, we nested a distinct serial number within the sampling site as a random effect to represent the paired design (coded as 1|sampling site/serial number, in the language of the R package *lme4*). To account for potential among-year variation, we also considered year as a crossed random factor. However, we considered year as a fixed factor for the models involving beetle population densities, which were collected from only two years. In all of the above models, we standardized non-categorical independent variables (i.e., elevation, temperature, forest cover, population density, beetle group size, blowfly abundance, Julian date, and year when considered in the fixed effect) to facilitate model convergence. We determined statistical significance using type II and type III sums of squares for non-interactive and interactive models, respectively, with the R package *car* (Fox & Weisberg, 2011). We calculated the R^2 for the LM using the R package Stats (R Core Team, 2022), and the marginal and conditional R^2 (R_m^2 and R_c^2) for the LMMs and GLMMs via the method described by Nakagawa & Schielzeth (Nakagawa & Schielzeth, 2013) using the R package *MuMIn* (Barton, 2020). We also informed the relative quality of the models by calculating the corrected Akaike information criterion (AIC_c) using the R package *MuMIn* (Barton, 2020).

In addition, we conducted pSEM to examine the potential causal relations among variables. The analysis compiles the above regression-based analyses through three major steps: (1) creating a hypothetical causal framework; (2) testing the goodness-of-fit of the hypothetical framework by d-sep tests (Shipley, 2009); and (3) testing the relationships among variables under the hypothetical framework (Lefcheck, 2016; Shipley, 2009). We also included the effect of blowfly abundance (log-transformed

to meet the normality assumption) which potentially modulates cooperation and reproductive success of beetles in the analysis. Furthermore, we also controlled for the influences of year and Julian date for the potential causal relations. For the parts of the pSEM involving beetle population density as a dependent variable, we also used log-transformed density and an LMM, instead of a negative binomial GLMM, to perform the analysis in order to obtain standardized coefficients for the potential causal relationships. We applied the same link function settings to all other parts of the pSEM as were used in the regression-based analyses. For any relationship involving a binary response (i.e., breeding success), the standardized coefficient was estimated manually following the approach proposed by Menard (Menard, 2004).

Sample sizes varied among analyses for reasons such as missing data due to lack of temperature monitoring, corresponding population density surveys, or lack of video recording in some experiments, as detailed in Appendix S1: Table S2. We used pairwise deletion for the LMM and GLMM models, excluding only samples with missing values for variables within each specific model. This approach aimed to maximize the sample size available for each analysis. However, to ensure uniformity across all components of the pSEM analysis—particularly regarding sample size—we applied listwise deletion, excluding all samples with any missing values. By comparing the outcomes of these two approaches, we can also evaluate the robustness of our statistical findings. We carried out all the above analyses using R version 4.2.1 (R Core Team, 2022).

Research permits

Permits for the field study were issued by Taiwan's Forestry Bureau (1014107656, 1024103748, 1034102881, and 1044105071 by Nantou Forest District Office; 1018106554, 1028101879, and 1038102225 by Hualien Forest District Office; 1013106573, 1023240523, 1033102695, and 1043103919 by Tungshih Forest District Office), and Taroko National Parks (201207310237, 201304120275, 201404090315, 201506020389) from 2012 to 2015.

RESULTS

IBM to simulate the impact of land-use change on realized thermal niches

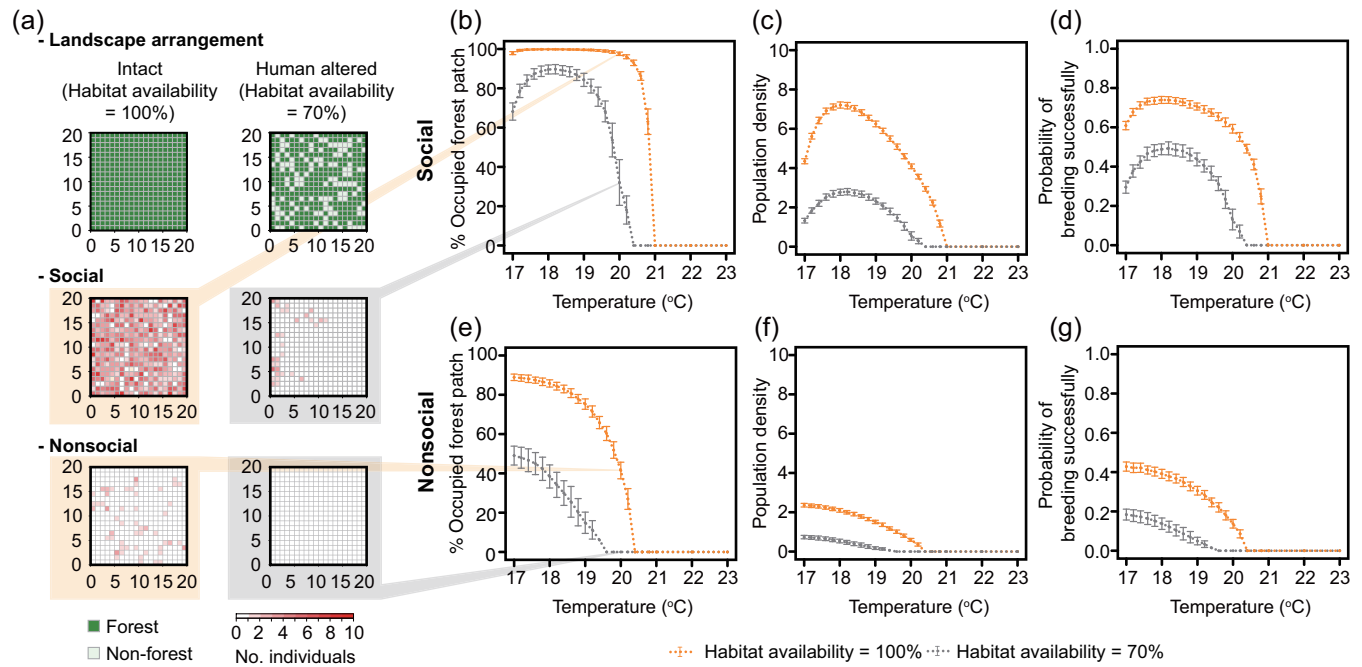Our IBM found that land-use change remarkably reduced the occupancy rate and population densities in the

FIGURE 3 Individual-based modeling for the impacts of land-use change on the realized thermal niche of social and nonsocial populations. (a) A pair of example landscapes (with different habitat availability) for the simulations, with a set of simulated results at the temperature of 20°C. Simulation results for patch occupation rate (b), population density (c), and probability of breeding successfully (d) along the temperature gradient in continuous and fragmented habitats in social species. Simulation results for patch occupation rate (e), population density (f), and probability of breeding successfully (g) along the temperature gradient in continuous and fragmented habitats in nonsocial species. In (a), each grid represents a habitat patch. In (b)–(g), points and error bars represent means and SDs obtained from 200 simulation runs.

remaining forest patches (Figure 3). Taking social organisms at 20°C as an example, a 30% loss of forest habitat led to a decrease in habitat occupancy from 97.5% to 32.0%, and population density dropped from 4.1 to 0.5 individuals (Figure 3a). In contrast, nonsocial organisms faced direct extinction from an initial 41.5% habitat occupancy and 0.6 individuals in population density (Figure 3a). Integrating simulation results across various temperatures, we found that the optimal temperature for social species in an intact landscape (forest habitat availability = 100%) was 18°C, with an upper temperature limit of 20.8°C. In a human-altered landscape (forest habitat availability = 70%), the optimal temperature was 18.2°C, with an upper limit of 20.2°C, indicating a thermal niche contraction. This was determined based on the number of occupied patches (Figure 3b), population density (Figure 3c), and the breeding performance of social species (Figure 3d). We also found that social species had larger cooperative group sizes in an intact forest landscape (Appendix S1: Figure S4). This phenomenon resulted in increased reproductive success due to higher population densities in intact forest compared with human-altered landscapes (see Appendix S1: Figure S5). For nonsocial species, the optimal temperature in both

intact and human-altered landscapes was below 17°C. However, the upper temperature limit was 20.2°C in intact forest and 19.4°C in human-altered landscapes, also suggesting a thermal niche contraction (Figure 3e–g).

Field study to examine the effect of land-use change on the population density, elevational range, and realized thermal niche of burying beetles

Forest cover and environmental temperature

Forest cover was significantly lower below 2500 m on the western slope compared with the eastern slope (LM; interaction Region × Elevation, Region × Elevation^2, and main effect of Region, all $p < 0.001$, $n = 72$; Appendix S1: Figure S6a, Table S3). Additionally, our analysis indicated that the mean daily temperature primarily decreased with increasing elevation, displaying a nearly consistent trend on both slopes (LMM; interaction Region × Elevation, $p = 0.09$; main effect of Region, $p = 0.29$, $n = 4849$; Appendix S1: Figure S6b, Table S4).

Notably, while a decrease in forest cover slightly intensified the elevational gradient of mean daily temperatures under the canopy (LMM; interaction Forest cover × Elevation, $p = 0.02$; main effect of Forest cover, $p = 0.88$, $n = 4849$; Appendix S1: Table S5a), the effect size of interaction between forest cover and elevation was small and did not contribute to either the R_m^2 or R_c^2 (Appendix S1: Table S5a,b), suggesting that forest cover had little influence on mean daily temperature.

Beetle population densities

To test the key predictions of the Habitat Loss-Allee Effect and Fixed Niche Breadth hypotheses, we compared the distribution and reproduction of *N. nepalensis* along the two elevational gradients. First, we investigated the difference in burying beetle population densities between the two slopes. At lower elevations, we noted significantly lower beetle densities on the western slope (GLMM; interaction Elevation × Region, $p = 0.03$, $n = 372$; Elevation equal to or below mean: Region, $p < 0.001$, $n = 192$; Appendix S1: Figure S7, Table S6a,b), which has undergone more extensive land-use change than the eastern slope. Conversely, at higher elevations with cooler temperatures, beetle densities were comparable between slopes (GLMM; Elevation above mean: Region, $p = 0.16$, $n = 180$; Appendix S1: Figure S7, Table S6c). Subsequently, the population densities between slopes also responded differently to temperature, with significantly lower densities on the western slope compared with the eastern slope at warmer temperatures (GLMM; interaction Temperature × Region, $p = 0.09$, $n = 372$; Temperature above mean: Region, $p = 0.01$, $n = 187$; Figure 4a; Appendix S1: Table S7).

We also tested whether the loss of forest cover is responsible for the lower beetle population density at lower elevations on the western slope. In regions with greater forest cover, we documented higher beetle densities (GLMM; Forest cover, $p < 0.001$, $n = 372$; Figure 4b; Appendix S1: Table S8a). However, the lower forest cover primarily contributed to the decreased population density at lower elevation (GLMM; interaction Elevation × Forest cover, $p = 0.001$, $n = 372$; Elevation equal to or below mean: GLMM; Forest cover, $p < 0.001$, $n = 192$; Appendix S1: Table S8a,b), but not at higher elevation (Elevation above mean: GLMM; Forest cover, $p = 0.74$, $n = 180$; Appendix S1: Table S8c). Notably, by statistically controlling for elevation, the effect of forest cover on beetle densities was similar on both the eastern and western slopes (GLMM; interaction Forest cover × Region, $p = 0.68$; Appendix S1: Table S9). Furthermore, by statistically accounting for the effect of forest cover, we found that the difference in beetle densities between slopes became non-significant (GLMM; interaction Elevation × Region, $p = 0.89$; main effect Region, $p = 0.43$, $n = 372$; Appendix S1: Table S9), suggesting that the variation in beetle population densities between slopes is primarily driven by forest cover.

We also compared the realized thermal niche of burying beetles, in terms of their distribution, on the two slopes with different degrees of land-use change. We found that the lower boundary of beetles on the western slope (1531 m, 20.0°C) was much higher than that on the eastern slope (1219 m, 22.8°C; Figure 4c). However, the upper boundary of the burying beetle distribution was similar on the two slopes (western: 2802 m, 12.5°C; eastern: 2873 m, 11.8°C; Figure 4c).

Beetle reproductive success

We conducted a set of field breeding experiments along the two elevational gradients to investigate how differences in population density caused by land-use change affect the reproductive thermal niche of burying beetles. We found that the higher beetle population density driven by a greater percentage of forest cover further improved beetle breeding performance at different temperatures (i.e., reproductive thermal niche). Thus, the reproductive success of burying beetles increased with increasing population density (GLMM; Population density, $p = 0.01$, $n = 322$; Figure 5a; Appendix S1: Table S10). In other words, high-density burying beetle populations had a higher probability of breeding successfully than low-density populations at the same temperature (Figure 5b; Appendix S1: Table S10). We further analyzed the behavioral mechanism of how population density affects the reproductive success of burying beetles and found that higher population densities resulted in larger cooperative groups than populations with lower densities at low elevations with higher temperatures (GLMM; interaction Population density × Temperature, $p = 0.001$; main effect of Population density, $p < 0.001$, $n = 199$; Figure 5c; Appendix S1: Table S11). In addition, higher beetle population densities also resulted in earlier carcass discoveries by the beetles (GLMM; interaction Population density × Temperature, $p = 0.07$; main effect of Population density, $p < 0.001$, $n = 210$; Figure 5d; Appendix S1: Table S12).

Finally, the pSEM analysis revealed the causal links between reduced forest cover and the reproductive success of burying beetles (Figure 5e, Appendix S1: Table S13). We identified four drivers of reduction in beetles' reproductive success: increased temperatures (pSEM; Temperature, $p < 0.001$, Appendix S1: Table S13), higher blowfly
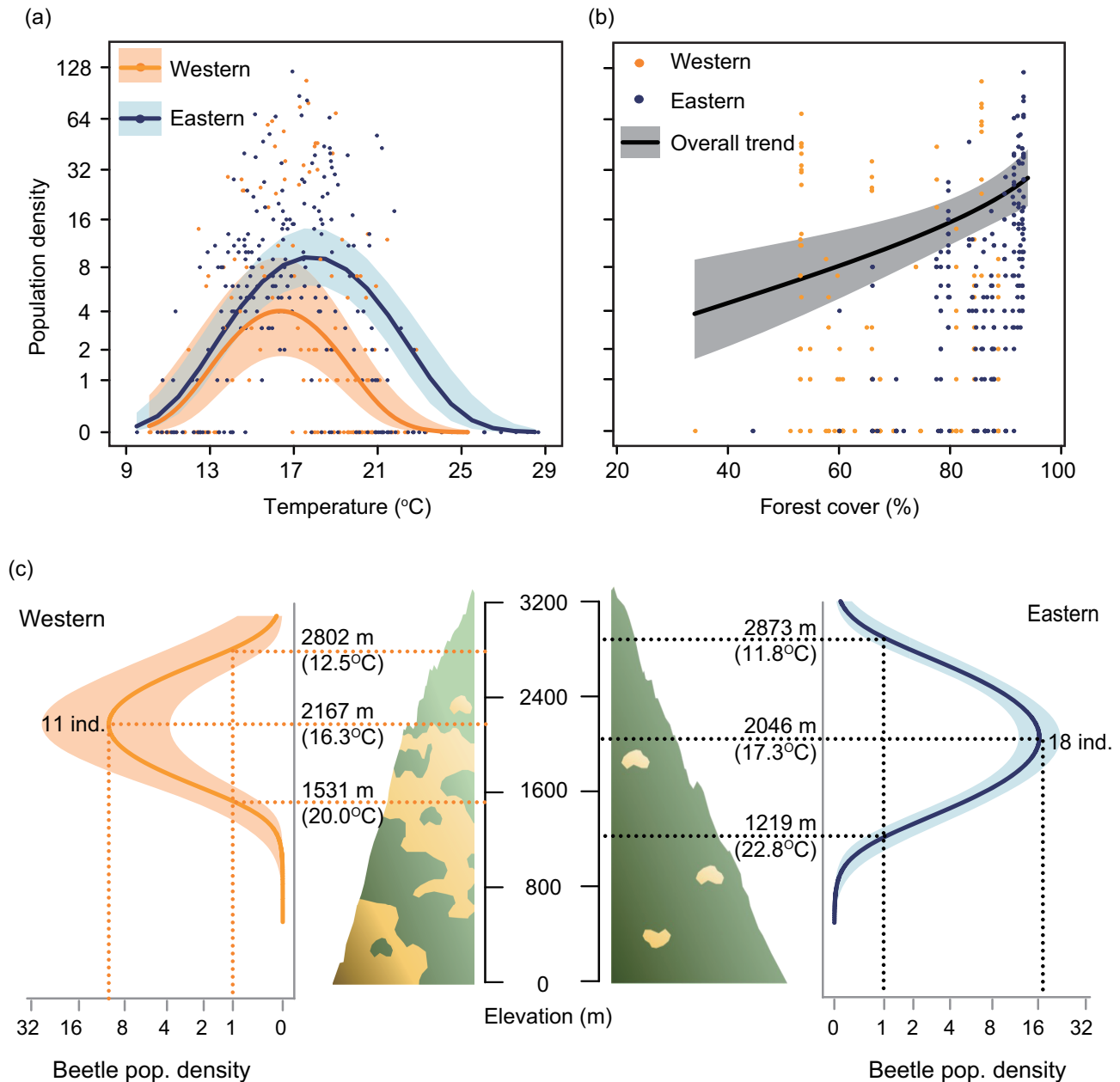
FIGURE 4 Population densities and elevational range boundaries of burying beetles. (a) The relationship between temperature and beetle population density along the eastern (intact) and western (human-altered) slopes. (b) The relationship between forest cover and beetle density. (c) The elevational range boundaries and population densities of burying beetles along the two slopes. All trends and 95% CIs (shaded areas) are estimated from generalized linear mixed models (GLMM). In (c), the upper elevational limit, the elevation with the highest population density, and the lower elevational limit for each slope are indicated by dashed lines. The upper and lower limits are the highest and lowest elevations at which the estimated population density (by GLMM) is no less than one individual.

abundances (pSEM; Blowfly abundance, $p < 0.01$, Appendix S1: Table S13), reduced beetle group sizes (pSEM; Beetle group size, $p < 0.01$, Appendix S1: Table S13), and prolonged periods to discover carcasses (pSEM; Beetle arrival day, $p < 0.001$, Appendix S1: Table S13). Of these, only the latter two were consequences of reduced population densities (pSEM; both $p < 0.001$, Appendix S1: Table S13).

Manipulative experiments for population density

We experimentally manipulated burying beetle group sizes to simulate the effect of changing beetle population densities to determine if population density impacts the beetles' reproductive thermal niche. We found that the probability of breeding successfully for larger groups
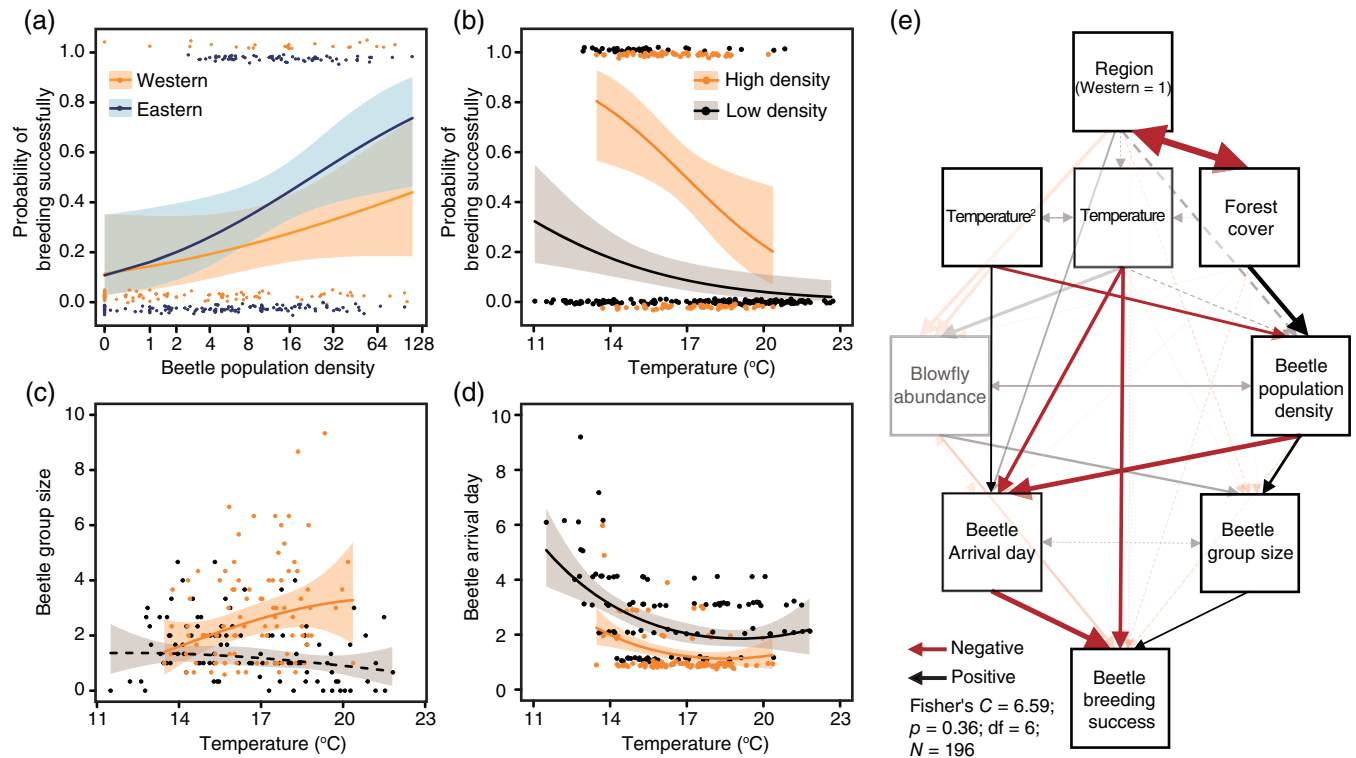
FIGURE 5 The influence of population density on burying beetle breeding success in field breeding experiments. (a) The influence of population density on beetle breeding success along the western and eastern slopes. (b) The influence of temperature on breeding success at high and low densities. (c) The influence of temperature on group size at high and low densities. (d) The influence of temperature on the arrival day of beetles, representing the day the beetles arrived at the carcass, at high and low densities. (e) Piecewise structural equation modeling (pSEM) for factors affecting breeding success of beetles. In (b)–(d), we considered a cutoff between high and low density at 11 individuals (the rounded mean value of all samples) for a better illustration of the results. All trends and 95% CIs (shaded areas) are estimated from generalized linear mixed models. In (a), (b), and (d), points are jittered along the vertical axes to avoid overplotting and improve readability. In (e), relationships of interest are highlighted with arrows in black (positive) and dark red (negative), whereas other potential relationships are shown with semitransparent arrows. Unidirectional arrows represent causal relationships, and bidirectional arrows represent correlational relationships. Numbers next to the arrows represent standardized coefficients. Arrows with solid lines are significant ($p < 0.05$), but those with dashed lines are not. The thickness of lines is proportional to the associated standardized coefficients. The influences of year and Julian date were statistically controlled in all causal relationships and were not shown in the figure. See Appendix S1: Table S9 for the summary of the pSEM.

(simulating group size at high population density) peaked at lower elevations (western: 2244 m; eastern: 2247 m; Figure 6a) and higher temperatures (western: 15.74°C; eastern: 15.24°C; Figure 6b,c), whereas the probability of breeding successfully for smaller groups (simulating group size at low population density) peaked at higher elevations (western: 2757 m; eastern: 2628 m; Figure 6a) and lower temperatures (western: 14.34°C; eastern: 13.64°C; Figure 6b,c). We also found that on both slopes, larger groups had higher reproductive success at low elevations (GLMM; interaction Elevation × Region × Treatment in the full model, $p = 0.37$; interaction Elevation × Treatment in the best model, $p < 0.01$, $n = 333$; Elevation equal to or below mean: Treatment, $p < 0.001$, $n = 185$; Figure 6a; Appendix S1: Table S14) and high temperatures (GLMM; interaction Temperature × Region × Treatment in the full model, $p = 0.99$; interaction Temperature × Treatment in

the best model, $p < 0.01$, $n = 333$; Temperature equal to or above mean: Treatment, $p = 0.02$, $n = 180$; Figure 6b,c; Appendix S1: Table S15).

DISCUSSION

Climate and land-use change drive the Allee effect and thermal niche contraction

Our combined theoretical and empirical results provide compelling evidence that land-use change significantly reshapes species' realized thermal niches through complex demographic processes, particularly the Allee effect. On the western slope of Mt. Hehuan, which has experienced greater land-use change, *N. nepalensis* exhibited lower reproductive success in the remnant pristine forest
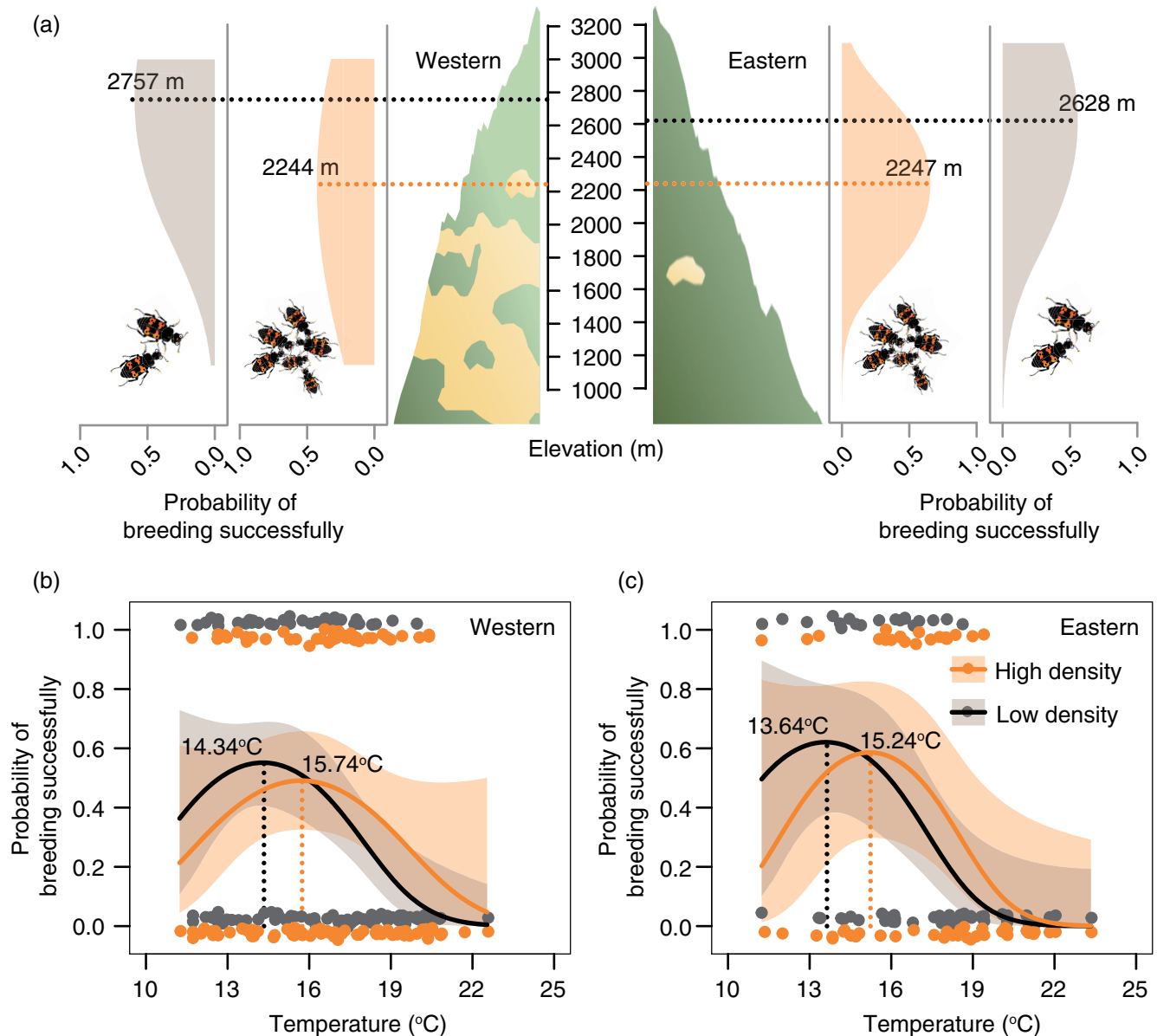
FIGURE 6 Field manipulative experiments for burying beetle population density. (a) Differences in elevational trends in reproductive success of beetles between treatments (high and low densities) and slopes (western and eastern). (b) The difference in thermal performances of beetles between treatments on the western slope. (c) The difference in thermal performance of beetles between treatments on the eastern slope. In a, the probability of breeding successfully was estimated by generalized linear mixed model (GLMM). Each horizontal dashed line indicates the elevation with the highest breeding success for each treatment and region. In (b) and (c), all trends and CIs (shaded areas) are estimated from GLMM. Vertical dashed lines indicate optimal temperatures, and points were jittered along the vertical axes to avoid overplotting and improve readability. Beetle illustration by Shih-Fan Chan.

compared with the eastern slope with intact forest, even at identical temperatures. Extensive exploitation of the western slope has driven a reduction in burying beetle population densities, leading to a contraction of the realized thermal niche. Consequently, the lower elevation limit of *N. nepalensis* has shifted approximately 300 m upward relative to the undisturbed eastern slope. In the context of land-use change, previous studies have primarily focused on comparing thermal tolerances between species in human-altered and natural habitats, often

assuming fixed, species-specific niches (Barnagaud et al., 2013; Frishkoff et al., 2015, 2019; Nowakowski et al., 2018; Piano et al., 2017; Williams & Newbold, 2020). Recent work has also identified variations in fundamental thermal niches due to local adaptations in urban environments, such as in Puerto Rican crested anoles (Campbell-Staton et al., 2020) and leaf-cutter ants (Angilletta et al., 2007). Furthermore, accumulating evidence suggests that realized thermal niches are dynamic and influenced by interspecific

interactions (Davis et al., 1998; Luhring & DeLong, 2016; Tsai, Rubenstein, Chen, et al., 2020). However, our study uniquely demonstrates how the Allee effect driven by land-use change, particularly in the context of cooperative group formation, influences a species' realized thermal niche. Taken together, our results support the Habitat Loss-Allee Effect hypothesis and reject the Fixed Niche Breadth hypothesis, highlighting the critical need to incorporate demographic effects when predicting species responses to climate and land-use change.

IBM predicts thermal niche contraction due to Allee effect

Our IBM demonstrates that land-use change contracts a species' realized thermal niche through the Allee effect. Despite a growing body of theoretical work on the impact of the Allee effect on ecological niches (Holt, 2009; Koffel et al., 2021), its specific role in shaping thermal niches has been overlooked. Previous models on the climate-driven Allee effect only incorporate temperature-dependent parameters such as growth rate, carrying capacity, attack rate, and handling time (Berec, 2019), life-history traits (Wittmann et al., 2011), and sex ratio (Berec et al., 2001), without considering the interactions between climate and land-use change. Our IBM addresses this gap by integrating frameworks from studies on environmental variation and cooperation (Chen et al., 2022; Lin et al., 2023), along with temperature-dependent parameters. The modeling results also extend recent theoretical findings that warming-induced resource reductions can reshape consumers' TPCs (Vinton & Vasseur, 2022), further demonstrating the joint effects of climate and land-use change leading to a contraction of the realized thermal niche.

Notably, our model of the social species demonstrated the loss of merely 30% of forest habitat at the relatively high temperature of 20°C resulted in a significant reduction in their elevational distribution and population density, as well as a substantial decrease in reproductive success (Figure 3a). This suggests that the impact of minor land-use changes will become substantial as temperatures rise. Such positive feedback mechanisms may further lead to extinction vortices (Fagan & Holmes, 2006; Soule, 1986), exacerbating species' vulnerability to global climate change. Interestingly, our IBM also showed a thermal niche contraction in nonsocial species. This suggests that land-use change can induce Allee effects in nonsocial species simply by reducing habitat and resource accessibility, such as that plants in lower population densities may experience reduced reproductive success due to their inability to attract sufficient pollinators (Groom, 1998). Overall, our modeling results highlight the complex interactions between climate and land-use change in shaping thermal niche dynamics, which further amplify climate impacts on species.

Behavioral modulation of Allee effect in burying beetles

In line with the IBM predictions, our field study shows that land-use change significantly affects *N. nepalensis*, leading to lower population densities and a contraction of its realized thermal niche. Further investigations have revealed the behavioral mechanisms underlying the suboptimal performance of *N. nepalensis* in warmer environments at low population densities. These include challenges in more quickly locating carcasses and forming larger cooperative groups, aligning with our IBM predictions that land-use change affects thermal niches through both resource accessibility and social behavior. While quickly locating carcasses helps to begin carcass processing earlier (Chan et al., 2019), forming large cooperative groups is critical for effectively removing maggots and burying carcasses (Chen et al., 2020; Liu et al., 2020; Sun et al., 2014; Tsai, Rubenstein, Chen, et al., 2020), both of which allow *N. nepalensis* to outcompete blowflies. These results bridge a critical knowledge gap, revealing that land-use change impacts thermal niches by affecting both thermal physiology and behaviors critical for reproduction. Consequently, our findings underscore the need to integrate physiological and behavioral approaches when predicting species' resilience to climate and land-use change.

Incorporating behavioral and demographic effects in addressing land-use and climate impacts on species resilience

In conclusion, our integrated approach combining theoretical modeling and field studies shows that land-use change can significantly reduce the breadth of realized thermal niches of species through complex mechanisms. These include reduced population densities and altered behaviors critical to reproduction, such as social interactions and resource location efficiency. Our results show that these effects are particularly pronounced in social species, although nonsocial species are also affected. These findings underscore the complex interactions between climate and land-use change, which may further exacerbate climate impacts by affecting species' population processes. To accurately assess species' vulnerability to these combined stressors, we propose a comprehensive framework that incorporates population dynamics,

demographic processes, and species-specific behaviors. This framework should assess: (1) how habitat affects population density; (2) how population density affects species fitness under different environmental conditions; and (3) whether and how conservation efforts can maintain population functioning under unfavorable climatic conditions. Practical measures should include the maintenance of abundant and well-connected habitats to support high population densities and improve accessibility to habitats and resources. For species with limited dispersal abilities, demographic restoration through artificial translocation (DeFilippo et al., 2022) can also promote resilience. Ultimately, integrating an understanding of species-specific behaviors and their population-level consequences with habitat conservation and the development of climate resilience measures is essential for conserving biodiversity in our rapidly changing world.

AUTHOR CONTRIBUTIONS

ACKNOWLEDGMENTS

CONFLICT OF INTEREST STATEMENT

The authors declare no conflicts of interest.

DATA AVAILABILITY STATEMENT

The C++ based program for the individual-based model (Chen, 2022) is available in Zenodo at https://doi.org/10.5281/zenodo.7039827. All data generated in this study and the R code for data analysis (Chan, Rubenstein, Wang, et al., 2023) are available in Figshare at https://doi.org/10.6084/m9.figshare.22586926.v6.

ORCID

Shih-Fan Chan https://orcid.org/0000-0003-2955-9433
Sheng-Feng Shen https://orcid.org/0000-0002-0631-6343

REFERENCES

Allee, W. C. 1927. "Animal aggregations." *The Quarterly Review of Biology* 2: 367–398.

Allee, W. C. 1931. *Animal Aggregations. A Study in General Sociology*. Chicago: The University of Chicago Press.

Angilletta, M. J., Jr., R. S. Wilson, A. C. Niehaus, M. W. Sears, C. A. Navas, and P. L. Ribeiro. 2007. "Urban Physiology: City Ants Possess High Heat Tolerance." *PLoS One* 2: e258.

Angulo, E., G. M. Luque, S. D. Gregory, J. W. Wenzel, C. Bessa-Gomes, L. Berec, and F. Courchamp. 2018. "Review: Allee Effects in Social Species." *The Journal of Animal Ecology* 87: 47–58.

Angulo, E., G. W. Roemer, L. Berec, G. Joanna, and F. Courchamp. 2007. "Double Allee Effects and Extinction in the Island Fox." *Conservation Biology* 21: 1082–91.

Barnagaud, J.-Y., L. Barbaro, A. Hampe, F. Jiguet, and F. Archaux. 2013. "Species' Thermal Preferences Affect Forest Bird Communities along Landscape and Local Scale Habitat Gradients." *Ecography* 36: 1218–26.

Barton, K. 2020. "MuMIn: Multi-Model Inference." R Package Version 1.43.17.

Bates, D., M. Maechler, B. Bolker, and S. Walker. 2015. "Fitting Linear Mixed-Effects Models Using lme4." *Journal of Statistical Software* 67: 1–48.

Berec, L. 2019. "Allee Effects under Climate Change." *Oikos* 128: 972–983.

Berec, L., D. S. Boukal, and M. Berec. 2001. "Linking the Allee Effect, Sexual Reproduction, and Temperature-Dependent Sex Determination Via Spatial Dynamics." *The American Naturalist* 157: 217–230.

Brook, B. W., N. S. Sodhi, and C. J. A. Bradshaw. 2008. "Synergies among Extinction Drivers under Global Change." *Trends in Ecology & Evolution* 23: 453–460.

Campbell-Staton, S. C., K. M. Winchell, N. C. Rochette, J. Fredette, I. Maayan, R. M. Schweizer, and J. Catchen. 2020. "Parallel Selection on Thermal Physiology Facilitates Repeated Adaptation of City Lizards to Urban Heat Islands." *Nature Ecology & Evolution* 4: 652–58.

Chan, S.-F., D. R. Rubenstein, I. C. Chen, Y.-M. Fan, H.-Y. Tsai, Y.-W. Zheng, and S.-F. Shen. 2023. "Higher Temperature Variability in Deforested Mountain Regions Impacts the Competitive Advantage of Nocturnal Species." *Proceedings of the Royal Society B* 290: 20230529.

Chan, S.-F., D. R. Rubenstein, T.-W. Wang, Y.-Y. Chen, I.-C. Chen, D.-Z. Ni, W.-K. Shih, and S.-F. Shen. 2023. "Source Data for: Land-Use Changes Influence Climate Resilience through Altered Population Demography in a Social Insect." Figshare. Dataset. https://doi.org/10.6084/m9.figshare.22586926.v6.

Chan, S.-F., W.-K. Shih, A.-Y. Chang, S.-F. Shen, and I. C. Chen. 2019. "Contrasting Forms of Competition Set Elevational Range Limits of Species." *Ecology Letters* 22: 1668–79.

Chan, B.-F., M. Liu, D. R. Rubenstein, S.-J. Sun, J.-N. Liu, Y.-H. Lin, and S.-F. Shen. 2020. "A Chemically Triggered Transition

from Conflict to Cooperation in Burying Beetles." *Ecology Letters* 23: 467–475.

Chen, I. C., J. K. Hill, R. Ohlemüller, D. B. Roy, and C. D. Thomas. 2011. "Rapid Range Shifts of Species Associated with High Levels of Climate Warming." *Science* 333: 1024–26.

Chen, Y. Y. 2022. "yychentw/Allee-Effect-Simulation: Allee Effects Mediate the Impact of Land-Use Change on the Thermal Niche of Social Species (v1.0.0)." Zenodo. https://doi.org/10.5281/zenodo.7039827.

Chen, Y.-Y., D. R. Rubenstein, and S.-F. Shen. 2022. "Cooperation and Lateral Forces: Moving beyond Bottom-Up and Top-Down Drivers of Animal Population Dynamics." *Frontiers in Psychology* 13: 768773.

Colwell Robert, K., and F. Rangel Thiago. 2009. "Hutchinson's Duality: The Once and Future Niche." *Proceedings of the National Academy of Sciences of the United States of America* 106: 19651–58.

Courchamp, F., T. Clutton-Brock, and B. Grenfell. 1999. "Inverse Density Dependence and the Allee Effect." *Trends in Ecology & Evolution* 14: 405–410.

Davis, A. J., L. S. Jenkinson, J. H. Lawton, B. Shorrocks, and S. Wood. 1998. "Making Mistakes When Predicting Shifts in Species Range in Response to Global Warming." *Nature* 391: 783–86.

DeFilippo, L. B., L. C. McManus, D. E. Schindler, M. L. Pinsky, M. A. Colton, H. E. Fox, E. W. Tekwa, S. R. Palumbi, T. E. Essington, and M. M. Webster. 2022. "Assessing the Potential for Demographic Restoration and Assisted Evolution to Build Climate Resilience in Coral Reefs." *Ecological Applications* 32: e2650.

Deutsch, C. A., J. J. Tewksbury, R. B. Huey, K. S. Sheldon, C. K. Ghalambor, D. C. Haak, and P. R. Martin. 2008. "Impacts of Climate Warming on Terrestrial Ectotherms across Latitude." *Proceedings of the National Academy of Sciences of the United States of America* 105: 6668–72.

Elsen, P. R., W. B. Monahan, and A. M. Merenlender. 2020. "Topography and Human Pressure in Mountain Ranges Alter Expected Species Responses to Climate Change." *Nature Communications* 11: 1974.

Fagan, W. F., and E. E. Holmes. 2006. "Quantifying the Extinction Vortex." *Ecology Letters* 9: 51–60.

Foley, J. A., R. DeFries, G. P. Asner, C. Barford, G. Bonan, S. R. Carpenter, F. S. Chapin, et al. 2005. "Global Consequences of Land Use." *Science* 309: 570–74.

Fox, J., and S. Weisberg. 2011. *An R Companion to Applied Regression*, 2nd ed. Thousand Oaks, CA: Sage.

Frishkoff, L. O., E. Gabot, G. Sandler, C. Marte, and D. L. Mahler. 2019. "Elevation Shapes the Reassembly of Anthropocene Lizard Communities." *Nature Ecology & Evolution* 3: 638–646.

Frishkoff, L. O., E. A. Hadly, and G. C. Daily. 2015. "Thermal Niche Predicts Tolerance to Habitat Conversion in Tropical Amphibians and Reptiles." *Global Change Biology* 21: 3901–16.

Groom, M. J. 1998. "Allee Effects Limit Population Viability of an Annual Plant." *The American Naturalist* 151: 487–496.

Grünbaum, D., and R. R. Veit. 2003. "Black-Browed Albatrosses Foraging on Antarctic Krill: Density-Dependence through Local Enhancement?" *Ecology* 84: 3265–75.

Guo, F., J. Lenoir, and T. C. Bonebrake. 2018. "Land-Use Change Interacts with Climate to Determine Elevational Species Redistribution." *Nature Communications* 9: 1315.

Haddad, N. M., L. A. Brudvig, J. Clobert, K. F. Davies, A. Gonzalez, R. D. Holt, T. E. Lovejoy, et al. 2015. "Habitat Fragmentation and its Lasting Impact on Earth's Ecosystems." *Science Advances* 1: e1500052.

Hansen, M. C., P. V. Potapov, R. Moore, M. Hancher, S. A. Turubanova, A. Tyukavina, D. Thau, et al. 2013. "High-Resolution Global Maps of 21st-Century Forest Cover Change." *Science* 342: 850–53.

Hof, C., I. Levinsky, M. B. AraÚJo, and C. Rahbek. 2011. "Rethinking Species' Ability to Cope with Rapid Climate Change." *Global Change Biology* 17: 2987–90.

Holt, R. D. 2009. "Bringing the Hutchinsonian Niche into the 21st Century: Ecological and Evolutionary Perspectives." *Proceedings of the National Academy of Sciences of the United States of America* 106: 19659–65.

Hutchinson, G. E. 1957. "Concluding Remarks." *Cold Spring Harbor Symposia on Quantitative Biology* 22: 415–427.

Jang, Y.-S., S.-F. Shen, J.-Y. Juang, C.-Y. Huang, and M.-H. Lo. 2022. "Discontinuity of Diurnal Temperature Range along Elevated Regions." *Geophysical Research Letters* 49: e2021GL097551.

Jarraud, M. 2008. *Guide to Meteorological Instruments and Methods of Observation* (WMO-No. 8). Geneva: World Meteorological Organisation.

Karger, D. N., O. Conrad, J. Böhner, T. Kawohl, H. Kreft, R. W. Soria-Auza, N. E. Zimmermann, H. P. Linder, and M. Kessler. 2017. "Climatologies at High Resolution for the Earth's Land Surface Areas." *Scientific Data* 4: 170122.

Koffel, T., T. Daufresne, and C. A. Klausmeier. 2021. "From Competition to Facilitation and Mutualism: A General Theory of the Niche." *Ecological Monographs* 91: e01458.

Lefcheck, J. S. 2016. "piecewiseSEM: Piecewise Structural Equation Modelling in r for Ecology, Evolution, and Systematics." *Methods in Ecology and Evolution* 7: 573–79.

Li, C.-F., M. Chytrý, D. Zelený, M.-Y. Chen, T.-Y. Chen, C.-R. Chiou, Y.-J. Hsia, et al. 2013. "Classification of Taiwan Forest Vegetation." *Applied Vegetation Science* 16: 698–719.

Lin, Y.-H., Y.-Y. Chen, D. R. Rubenstein, M. Liu, M. Liu, and S.-F. Shen. 2023. "Environmental Quality Mediates the Ecological Dominance of Cooperatively Breeding Birds." *Ecology Letters* 26: 1145–56.

Liu, M., S.-F. Chan, D. R. Rubenstein, S.-J. Sun, B.-F. Chen, and S.-F. Shen. 2020. "Ecological Transitions in Grouping Benefits Explain the Paradox of Environmental Quality and Sociality." *The American Naturalist* 195: 818–832.

Luhring, T. M., and J. P. DeLong. 2016. "Predation Changes the Shape of Thermal Performance Curves for Population Growth Rate." *Current Zoology* 62: 501–5.

Menard, S. 2004. "Six Approaches to Calculating Standardized Logistic Regression Coefficients." *The American Statistician* 58: 218–223.

Nakagawa, S., and H. Schielzeth. 2013. "A General and Simple Method for Obtaining R^2 from Generalized Linear Mixed-Effects Models." *Methods in Ecology and Evolution* 4: 133–142.

Newbold, T., L. N. Hudson, S. L. L. Hill, S. Contu, I. Lysenko, R. A. Senior, L. Börger, et al. 2015. "Global Effects of Land Use on Local Terrestrial Biodiversity." *Nature* 520: 45–50.

Nowakowski, A. J., L. O. Frishkoff, M. E. Thompson, T. M. Smith, and B. D. Todd. 2018. "Phylogenetic Homogenization of

Amphibian Assemblages in Human-Altered Habitats across the Globe." *Proceedings of the National Academy of Sciences of the United States of America* 115: E3454–E3462.

Oliver, T. H., H. H. Marshall, M. D. Morecroft, T. Brereton, C. Prudhomme, and C. Huntingford. 2015. "Interacting Effects of Climate Change and Habitat Fragmentation on Drought-Sensitive Butterflies." *Nature Climate Change* 5: 941–45.

Oliver, T. H., and M. D. Morecroft. 2014. "Interactions between Climate Change and Land Use Change on Biodiversity: Attribution Problems, Risks, and Opportunities." *Wiley Interdisciplinary Reviews: Climate Change* 5: 317–335.

Parmesan, C. 2006. "Ecological and Evolutionary Responses to Recent Climate Change." *Annual Review of Ecology, Evolution, and Systematics* 37: 637–669.

Parmesan, C., and G. Yohe. 2003. "A Globally Coherent Fingerprint of Climate Change Impacts across Natural Systems." *Nature* 421: 37–42.

Pecl, G. T., M. B. Araújo, J. D. Bell, J. Blanchard, T. C. Bonebrake, I. C. Chen, T. D. Clark, et al. 2017. "Biodiversity Redistribution under Climate Change: Impacts on Ecosystems and Human Well-Being." *Science* 355: eaai9214.

Peters, M. K., A. Hemp, T. Appelhans, J. N. Becker, C. Behler, A. Classen, F. Detsch, et al. 2019. "Climate–Land-Use Interactions Shape Tropical Mountain Biodiversity and Ecosystem Functions." *Nature* 568: 88–92.

Piano, E., K. De Wolf, F. Bona, D. Bonte, D. E. Bowler, M. Isaia, L. Lens, et al. 2017. "Urbanization Drives Community Shifts towards Thermophilic and Dispersive Species at Local and Landscape Scales." *Global Change Biology* 23: 2554–64.

Platts, P. J., S. C. Mason, G. Palmer, J. K. Hill, T. H. Oliver, G. D. Powney, R. Fox, and C. D. Thomas. 2019. "Habitat Availability Explains Variation in Climate-Driven Range Shifts across Multiple Taxonomic Groups." *Scientific Reports* 9: 15039.

R Core Team. 2022. *R: A Language and Environment for Statistical Computing*. R Package Version 4.2.1. Vienna: R Foundation for Statistical Computing.

Schulte to Bühne, H., J. A. Tobias, S. M. Durant, and N. Pettorelli. 2021. "Improving Predictions of Climate Change–Land Use Change Interactions." *Trends in Ecology & Evolution* 36: 29–38.

Scott, M. P. 1994. "Competition with Flies Promotes Communal Breeding in the Burying Beetle, *Nicrophorus tomentosus*." *Behavioral Ecology and Sociobiology* 34: 367–373.

Scott, M. P. 1998. "The Ecology and Behavior of Burying Beetles." *Annual Review of Entomology* 43: 595–618.

Senior, R. A., J. K. Hill, and D. P. Edwards. 2019. "Global Loss of Climate Connectivity in Tropical Forests." *Nature Climate Change* 9: 623–26.

Shipley, B. 2009. "Confirmatory Path Analysis in a Generalized Multilevel Context." *Ecology* 90: 363–68.

Soule, M. E. 1986. *Conservation Biology—The Science of Scarcity and Diversity*. Sunderland, MA: Sinauer Associates.

Stephens, P. A., and W. J. Sutherland. 1999. "Consequences of the Allee Effect for Behaviour, Ecology and Conservation." *Trends in Ecology & Evolution* 14: 401–5.

Sun, S.-J., D. R. Rubenstein, B.-F. Chen, S.-F. Chan, J.-N. Liu, M. Liu, W. Hwang, P.-S. Yang, and S.-F. Shen. 2014.

"Climate-Mediated Cooperation Promotes Niche Expansion in Burying Beetles." *eLife* 3: e02440.

Travis, J. M. J. 2003. "Climate Change and Habitat Destruction: A Deadly Anthropogenic Cocktail." *Proceedings of the Royal Society of London B* 270: 467–473.

Tsai, H.-Y., D. R. Rubenstein, B.-F. Chen, M. Liu, S.-F. Chan, D.-P. Chen, S.-J. Sun, T.-N. Yuan, and S.-F. Shen. 2020. "Antagonistic Effects of Intraspecific Cooperation and Interspecific Competition on Thermal Performance." *eLife* 9: e57022.

Tsai, H.-Y., D. R. Rubenstein, Y.-M. Fan, T.-N. Yuan, B.-F. Chen, Y. Tang, I. C. Chen, and S.-F. Shen. 2020. "Locally-Adapted Reproductive Photoperiodism Determines Population Vulnerability to Climate Change in Burying Beetles." *Nature Communications* 11: 1398.

Tucker, M. A., K. Böhning-Gaese, W. F. Fagan, J. M. Fryxell, B. Van Moorter, S. C. Alberts, A. H. Ali, et al. 2018. "Moving in the Anthropocene: Global Reductions in Terrestrial Mammalian Movements." *Science* 359: 466–69.

Vasseur, D. A., J. P. DeLong, B. Gilbert, H. S. Greig, C. D. Harley, K. S. McCann, V. Savage, T. D. Tunney, and M. I. O'Connor. 2014. "Increased Temperature Variation Poses a Greater Risk to Species than Climate Warming." *Proceedings of the Royal Society B* 281: 20132612.

Vinton, A. C., and D. A. Vasseur. 2022. "Resource Limitation Determines Realized Thermal Performance of Consumers in Trophodynamic Models." *Ecology Letters* 25: 2142–55.

Wells, H., E. G. Strauss, M. A. Rutter, and P. H. Wells. 1998. "Mate Location, Population Growth and Species Extinction." *Biological Conservation* 86: 317–324.

Williams, J. J., and T. Newbold. 2020. "Local Climatic Changes Affect Biodiversity Responses to Land Use: A Review." *Diversity and Distributions* 26: 76–92.

Wilson, E. O. 1975. *Sociobiology: The New Synthesis*. Cambridge, MA: Harvard University Press.

Wittmann, M. J., M. A. Lewis, J. D. Young, and N. D. Yan. 2011. "Temperature-Dependent Allee Effects in a Stage-Structured Model for Bythotrephes Establishment." *Biological Invasions* 13: 2477–97.

SUPPORTING INFORMATION

Additional supporting information can be found online in the Supporting Information section at the end of this article.